Journal of Geothermal Research and Volcanology (2026) 27-35

Contents lists available at FoundAE

Journal of Geothermal Research and Volcanology

Journal homepage: https://ejournal.foundae.com/index.php/jograv/index

Integrated 2D–3D gravity modeling reveals structural controls of a granite-hosted non-volcanic geothermal system in West Kalimantan, Indonesia

Succi Angling Situmorang[a,*], Ahmad Said[b]

[a] Department of Physics, Institut Teknologi Sumatera, Way Huwi, Jati Agung, South Lampung, Lampung 35365, Indonesia
[b] Friedrich-Schiller-University Jena, Friedrich-Schellingstr, 07745 Jena, Germany

ARTICLE INFO

Keywords:
Non-volcanic
geothermal exploration
Gravity inversion
Crustal heat production
Granite intrusion
Granite-hosted

ABSTRACT

West Kalimantan, Indonesia, forms part of a granitic province associated with the Southeast Asian tin belt, characterized by felsic intrusions enriched in heat-producing elements such as uranium (U), thorium (Th), and potassium (K). The radiogenic decay of these elements may contribute to localized crustal heat accumulation, suggesting potential for non-volcanic geothermal systems. The Meromoh geothermal area is one such manifestation suspected to be structurally controlled by underlying granitic bodies. However, the subsurface architecture and the geometry of potential heat sources remain poorly constrained. This study aims to characterize the subsurface structure of the Meromoh geothermal system using satellite-derived gravity data integrated with two-dimensional (2D) forward modeling and three-dimensional (3D) inversion. Secondary datasets including longitude, latitude, elevation, and Free-Air Anomaly (FAA) were obtained from the TOPEX global gravity database and processed to generate a Complete Bouguer Anomaly (CBA) map. The CBA values range from 15.8 to 61.7 mGal, indicating significant subsurface density contrasts across the study area. The integrated modeling results reveal a crustal structure composed of the Kayan Sandstone Formation, Pendawan Formation, Dasit and Bawang units, and the Pueh Granite Formation. The Pueh Granite is interpreted as a deep-seated intrusive body extending from near-surface levels to a depth of approximately 11.6 km. Structural discontinuities and density contrasts suggest that the granite intrusion plays a key role in controlling geothermal manifestations. These findings provide new geophysical constraints on granite-hosted geothermal systems in West Kalimantan and highlight the importance of gravity-based structural modeling for evaluating non-volcanic geothermal potential in radiogenic provinces.

1. Introduction

Geothermal energy represents one of the most reliable and sustainable renewable energy resources, capable of delivering continuous baseload power with relatively low greenhouse gas emissions compared to fossil fuels. While geothermal development has traditionally focused on high-enthalpy volcanic systems associated with active magmatism, increasing attention has been directed toward non-volcanic geothermal systems occurring in tectonically stable or post-magmatic environments. These systems are typically characterized by moderate temperature regimes and are often controlled by crustal architecture, permeability structures, and long-term heat accumulation rather than shallow magmatic intrusions [1, 2].

Among non-volcanic geothermal environments, granite-hosted systems have attracted growing interest. Granitic intrusions commonly contain elevated concentrations of heat-producing elements such as uranium (U), thorium (Th), and potassium (K), whose radioactive decay contributes to sustained crustal heat production over geological timescales [3–5]. In regions where granitic bodies are voluminous and structurally interconnected, cumulative radiogenic heat may elevate local geothermal gradients and support hydrothermal circulation in the absence of active volcanism [6, 7]. However, the viability of such systems depends strongly on subsurface geometry, depth extent of the intrusive bodies, and the presence of structural pathways that enable fluid circulation [8–10].

* Corresponding author.
E-mail address: succiangling@gmail.com (S. A. Situmorang).

https://doi.org/10.58524/jograv.v1i1.107
Received 6 January 2026; Received in revised form 12 February 2026; Accepted 15 February 2026
Available online 5 March 2026
XXXX-XXXX/Published by FoundAE (Foundation of Advanced Education).

The identification and characterization of granite-hosted non-volcanic geothermal systems pose significant exploration challenges. Unlike volcanic systems, where heat sources are often shallow and geophysically conspicuous, radiogenic or deep-seated granitic heat sources may produce subtler thermal anomalies. Surface manifestations, such as warm springs, may reflect structurally controlled fluid flow rather than direct proximity to a magmatic heat source. Consequently, constraining the crustal architecture and structural controls becomes essential for evaluating geothermal potential in such settings [3, 11].

West Kalimantan, located in the western part of Borneo Island, Indonesia, forms part of a granitic province associated with the Southeast Asian tin belt. This metallogenic belt is characterized by widespread felsic intrusions emplaced during Late Paleozoic to Mesozoic tectono-magmatic events. The granitic bodies in this region are geochemically evolved and regionally associated with mineralization, suggesting enrichment in incompatible elements. Although geothermal exploration in Indonesia has predominantly targeted volcanic arcs along Sumatra, Java, and Sulawesi, non-volcanic geothermal occurrences have been reported in granitic terrains, including the Meromoh geothermal area in West Kalimantan (Fig. 1) [12, 13].

The Meromoh area exhibits surface geothermal manifestations in the form of warm springs, yet it lies outside the active volcanic arc. The absence of Quaternary volcanism indicates that the geothermal system is unlikely to be magmatically driven. Instead, the system is hypothesized to be structurally controlled and potentially associated with underlying granitic intrusions. However, the subsurface configuration of these intrusions, their depth extent, and their relationship to regional fault systems remain poorly constrained. Without detailed structural characterization, the role of granite bodies in sustaining geothermal circulation cannot be adequately assessed.

Geophysical methods offer an effective approach for investigating subsurface structures in regions where drilling data are limited. Among these methods, gravity surveying is particularly suitable for mapping density contrasts associated with intrusive bodies, sedimentary basins, and basement architecture [6, 14, 15]. Granitic rocks typically exhibit higher densities compared to sedimentary units, enabling their detection through gravity anomaly analysis. When combined with quantitative modeling techniques, gravity data can provide insights into the geometry and depth distribution of intrusive bodies and structural discontinuities that may act as geothermal conduits [4, 16].

Despite its advantages, gravity interpretation is inherently non-unique. Therefore, integrated approaches that combine two-dimensional (2D) forward modeling and three-dimensional (3D) inversion are increasingly employed to improve model robustness and reduce ambiguity. 2D forward modeling allows detailed examination of subsurface geometry along selected profiles, constrained by geological information, while 3D inversion provides volumetric density distribution across the broader study area. The integration of these methods enhances confidence in structural interpretation and enables a more comprehensive understanding of crustal architecture [17, 18].

Previous geothermal studies in Indonesia have largely focused on volcanic systems, emphasizing magmatic heat sources and shallow reservoirs. In contrast, granite-hosted geothermal systems in tectonically stable or post-magmatic provinces remain underexplored [19–21]. In West Kalimantan, existing studies have primarily addressed regional geology and mineralization, with limited attention to subsurface structural controls relevant to geothermal processes. As a result, the structural framework governing the Meromoh geothermal manifestation has not been quantitatively evaluated using integrated geophysical modeling [1].

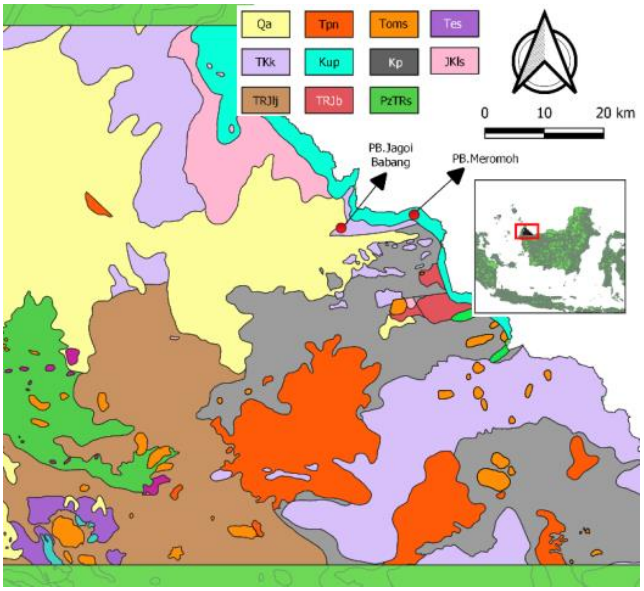

Fig. 1. Regional geological in the Meromoh geothermal area, located in Bengkayang Regency, West Kalimantan, Indonesia, within the geographic coordinates of 0°54′–1°40′ N and 109°17′–110°27′ E.

This study aims to characterize the subsurface structure and structural controls of the Meromoh geothermal system in West Kalimantan using satellite-derived gravity data integrated with 2D forward modeling and 3D inversion. Specifically, the objectives are to: (1) delineate density contrasts associated with granitic intrusions and surrounding formations; (2) estimate the depth extent and geometry of intrusive bodies beneath the geothermal manifestation area; and (3) assess the role of structural discontinuities in controlling geothermal fluid circulation. By integrating Complete Bouguer Anomaly mapping with spectral analysis and multi-scale modeling, this study provides quantitative constraints on the crustal architecture of a granite-hosted non-volcanic geothermal system [3, 6, 16].

The findings contribute to a broader understanding of geothermal processes in radiogenic and post-magmatic provinces, where heat sources are less obvious than in volcanic environments. Furthermore, the study demonstrates the applicability of integrated gravity modeling as a first-order exploration tool for structurally controlled geothermal systems in data-limited regions. By refining the subsurface structural model of the Meromoh area, this work supports more informed assessment of non-volcanic geothermal potential in West Kalimantan and similar granitic provinces worldwide.

2. Conceptual geological setting

The Meromoh geothermal area is located in Bengkayang Regency, West Kalimantan, Indonesia, within the coordinate range of 0°54′–1°40′ N and 109°17′–110°27′ E. The study area lies within the southwestern segment of Borneo Island and forms part of the broader granitic province associated with the Southeast Asian tin belt. This tectono-magmatic province is characterized by widespread felsic intrusions emplaced during Late Triassic to Early Cretaceous time, particularly within the Schwaner Mountains region [6, 14, 15].

Regionally, West Kalimantan represents a stable continental block composed of crystalline basement intruded by granitic plutons and overlain by sedimentary successions. The granitic intrusions are predominantly S-type to highly evolved felsic bodies, commonly associated with mineralization and enrichment in incompatible elements. These granites form extensive batholiths and intrusive complexes that locally crop out at the surface and are interpreted to extend to mid-crustal depths. Their emplacement reflects post-collisional to extensional tectonic processes following Paleozoic–Mesozoic convergence along the Sundaland margin [3, 6, 16].

Structurally, the Meromoh area is influenced by NW–SE and NE–SW trending fault systems that are regionally developed across West Kalimantan. Major lineaments such as the Sintang Fault Zone (SFZ) and related subsidiary structures are interpreted to represent long-lived crustal discontinuities. These fault systems likely originated from regional tectonic deformation and were subsequently reactivated during post-magmatic crustal adjustment. The intersection between intrusive contacts and fault zones creates mechanical contrasts and permeability pathways that are favorable for hydrothermal circulation [19–21].

The local stratigraphy in the Meromoh area consists of sedimentary formations including the Kayan Sandstone Formation and Pendawan Formation, intercalated with volcanic and intrusive units such as Dasit, Bawang, and the Pueh Granite Formation. The sedimentary units are composed predominantly of sandstone, shale, and minor volcaniclastic deposits, which may act as secondary permeability zones when fractured. In contrast, the granitic bodies form the crystalline basement and are interpreted to represent the primary intrusive framework controlling crustal heat distribution.

Geothermal manifestations in the Meromoh area are characterized by the presence of warm springs with measured surface temperatures of approximately 29°C. Although the observed temperature is relatively low compared to high-enthalpy volcanic systems, it indicates active hydrothermal circulation. The absence of Quaternary volcanic activity suggests that the geothermal system is non-volcanic in origin and is likely governed by long-term crustal heat and structurally controlled fluid flow rather than shallow magmatic intrusion.

A conceptual geological model of the Meromoh geothermal system can therefore be proposed. In this model, granitic intrusions at depth constitute the primary crustal heat source. Heat is transferred upward through conduction within the crystalline basement and is locally enhanced by convective circulation along fault-controlled permeability zones. Meteoric water infiltrates through fractured sedimentary formations and structural discontinuities, descends to depth where it is heated, and subsequently ascends along fault intersections, discharging as warm springs at the surface.

The effectiveness of this geothermal system depends on several key geological factors: (1) the thickness and lateral continuity of the granitic intrusions, (2) the depth extent of the intrusive bodies, (3) the presence of structurally enhanced permeability zones, and (4) the hydraulic connectivity between granite–sediment interfaces. The interaction between intrusive geometry and fault architecture is therefore critical in controlling the localization of geothermal manifestations in the Meromoh area. This conceptual geological framework provides the basis for interpreting gravity-derived subsurface density contrasts and evaluating the structural controls of the granite-hosted non-volcanic geothermal system in West Kalimantan [19–21].

3. Method

3.1. Study area and data source

The study was conducted in the Meromoh geothermal area, located in Bengkayang Regency, West Kalimantan, Indonesia, within the geographic coordinates of 0°54′–1°40′ N and 109°17′–110°27′ E (Fig. 1). The investigation was carried out between October 2022 and March 2023 through data processing and modeling activities conducted at the Earth Physics Laboratory, Physics Study Program, Institut Teknologi Sumatera.

The Meromoh geothermal system is characterized by surface manifestations in the form of warm springs with measured temperatures of approximately 29°C. The absence of Quaternary volcanic activity suggests that the system is structurally controlled and potentially associated with deeper crustal heat sources.

This study utilized secondary gravity and topographic datasets derived from satellite observations. Free-Air Anomaly (FAA), geographic coordinates (longitude and latitude), and elevation data were obtained from the TOPEX/UCSD global gravity database (https://topex.ucsd.edu/cgi-bin/get_data.cgi).

The dataset was extracted on 10 October 2022 using the defined geographic boundaries of the Meromoh area. The extracted data were provided in ASCII XYZ format, consisting of regularly gridded latitude, longitude, elevation, and FAA values. To perform terrain correction, Shuttle Radar Topography Mission (SRTM) data were obtained from the United States Geological Survey (USGS). The SRTM dataset was processed using Global Mapper to generate topographic grids in Surfer Grid format for terrain correction calculations. Regional geological maps were used to constrain lithological interpretation and guide density assignment during modeling.

3.2. Gravity data processing

Initial data processing was conducted in Microsoft Excel 2019. The FAA and elevation datasets were combined into a single database for correction calculations. The Complete Bouguer Anomaly (CBA) was calculated through the following steps:

1. Free-air correction (already included in FAA data).
2. Bouguer correction using an estimated average rock density.
3. Terrain correction to remove topographic effects.

The Bouguer correction was applied to obtain the Simple Bouguer Anomaly (SBA) [14, 22, 23] using equation (1).

$$\Delta g_B = \Delta g_{FA} - (0.04193\rho h) \quad \ldots (1)$$

where ρ is the Bouguer density (g/cm³) and h is elevation (m).

Optimal Bouguer density was determined through correlation analysis between gravity anomaly and elevation values. The density value minimizing correlation was selected as the representative surface density. Terrain correction was performed in Oasis Montaj using SRTM-derived elevation data. The terrain correction values were then added to the SBA to obtain the (CBA) was calculated as equation (2).

$$CBA = FAA - Bouguer\ Correction + Terrain\ Correction \quad \ldots (2)$$

The corrected dataset was subsequently converted into UTM Zone 48S coordinates for spatial analysis.

3.3. Spectral analysis and regional–residual separation

Spectral analysis was performed in Oasis Montaj to estimate the average depth of gravity anomaly sources and to separate regional and residual components. The Fourier transform was applied to the CBA dataset, converting spatial-domain gravity data into the frequency (wavenumber) domain in equation (3).

$$F(k) = \int_{-\infty}^{\infty} f(x) e^{-ikx} dx \quad \ldots (3)$$

The logarithmic power spectrum was plotted as log amplitude versus wavenumber. The slope of linear segments was used to estimate source depth, where steeper slopes correspond to deeper sources and gentler slopes indicate shallower structures. Regional and residual anomalies were separated using frequency-domain filtering:

- Low-pass filter → isolates deep regional anomalies
- Band-pass filter → highlights shallow residual anomalies

Residual anomalies are interpreted to represent shallow density contrasts related to structural features and geothermal circulation pathways.

3.4. Two and three-dimensional forward modeling

Two-dimensional forward modeling was conducted along selected profiles crossing significant gravity anomalies. The objective was to estimate subsurface geometry and density distribution consistent with observed gravity responses. Modeling was performed using Oasis Montaj, integrating geological constraints. A trial-and-error forward modeling approach was applied until the misfit between observed and calculated anomalies was minimized (error <5%). The minimum and maximum density values obtained from 2D modeling were used as constraints for subsequent 3D inversion modeling.

Three-dimensional gravity modeling was performed using Grablox 1.6e, with visualization in Bloxer 1.6e. The workflow consisted of:

1. Initial Forward Modeling
   A block model representing the study area was constructed based on gridded Complete Bouguer Anomaly data. Major and minor blocks were defined according to spatial resolution and area extent.
2. Density Parameter Assignment
   Density values derived from 2D modeling were assigned as initial constraints.
3. Inverse Modeling
   An iterative inversion procedure was applied to adjust density distribution and geometry to minimize misfit between observed and calculated gravity anomalies. Optimization stages included:
   - Base model adjustment
   - Density optimization
   - Occam density smoothing
   - Elevation adjustment
   - Occam height smoothing

The inversion process aimed to reduce residual error and obtain a geologically reasonable subsurface density model.

3.5. *Data interpretation*

Interpretation was conducted qualitatively and quantitatively. For the qualitative interpretation, gravity anomaly maps (Complete Bouguer, regional, and residual) were analyzed to identify patterns associated with density contrasts. High gravity anomalies were interpreted as potential granitoid intrusions or basement highs, whereas low residual anomalies were interpreted as fractured or altered zones possibly associated with geothermal fluid pathways.

While quantitative interpretation, the cross-sectional models from 2D forward modeling and volumetric density distributions from 3D inversion were integrated with geological maps. Density contrasts were correlated with lithological units and structural features, particularly fault systems that may act as geothermal conduits. The final interpretation focuses on identifying:

- Potential granite heat sources
- Structural controls (faults/fractures)
- Zones of reduced density indicative of hydrothermal alteration

4. Results and discussion

4.1. *Complete bouguer anomaly (CBA) map*

The Complete Bouguer Anomaly (CBA) map represents subsurface density variations derived from corrected gravity data. After applying free-air, Bouguer, and terrain corrections, the resulting anomaly reflects contrasts in rock density beneath the surface. The processed data were projected in UTM Zone 48N coordinates, with anomaly values ranging from 15.8 mGal to 61.7 mGal (Fig. 2).

The spatial distribution of CBA values reveals significant lateral density contrasts across the study area. High anomaly zones are predominantly observed in the central and southern parts of the map, whereas relatively lower anomalies occur toward the northeastern and localized western sectors. These variations are interpreted to reflect differences in lithological composition and subsurface structural configuration [24].

The Meromoh geothermal manifestation is situated within an area characterized by relatively elevated gravity anomaly values and corresponds spatially with the Pueh Granite Formation. This formation consists primarily of granite, granodiorite, and diorite, lithologies that typically exhibit higher densities compared to surrounding sedimentary units. The presence of high gravity anomalies in this zone is therefore consistent with the distribution of intrusive crystalline rocks at shallow to intermediate depths.

In contrast, the Jagoi Babang geothermal occurrence is located within the Kayan Sandstone Formation, composed mainly of quartz sandstone with minor mudstone and conglomerate intercalations. These sedimentary units generally exhibit lower densities than intrusive granitoids. However, localized gravity highs near Jagoi Babang suggest possible basement uplift, shallow intrusive contacts, or structural control influencing subsurface density distribution. Gravity anomaly values can be broadly classified into three categories within the study area:

- Low anomalies (15.8–31.2 mGal), interpreted as relatively lower-density zones that may correspond to sedimentary accumulations or structurally fractured regions.
- Intermediate anomalies (31.6–34.1 mGal), representing transitional density contrasts between sedimentary and crystalline units.
- High anomalies (34.6–61.7 mGal), associated with high-density intrusive bodies or basement highs.

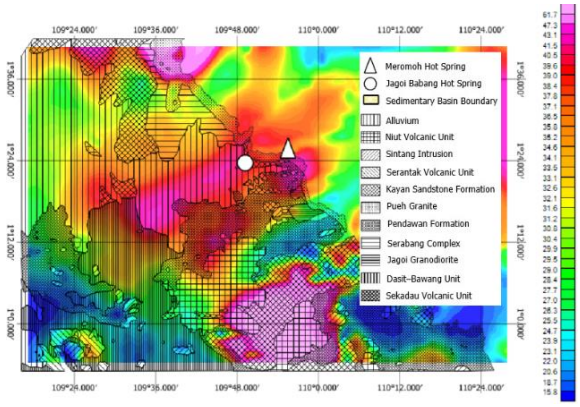

Fig. 2. Complete bouguer anomaly (CBA) map in the Meromoh geothermal area, West Kalimantan, Indonesia.

It is important to note that high gravity anomaly values do not directly confirm the presence of a geothermal heat source. Instead, they indicate the existence of dense subsurface materials, which in this geological context are interpreted as granitoid intrusions. The relationship between these dense bodies and geothermal manifestations suggests that intrusive geometry and associated structural discontinuities may play a critical role in controlling hydrothermal circulation.

The coincidence between elevated gravity anomalies and geothermal manifestations in the Meromoh area implies that the granite intrusion likely contributes to the thermal regime of the system. However, the development of surface hot springs is also strongly dependent on fault-controlled permeability pathways rather than solely on density contrasts. Therefore, integration with structural analysis and subsequent 2D–3D modeling is necessary to better constrain the geometry and depth extent of the interpreted intrusive bodies.

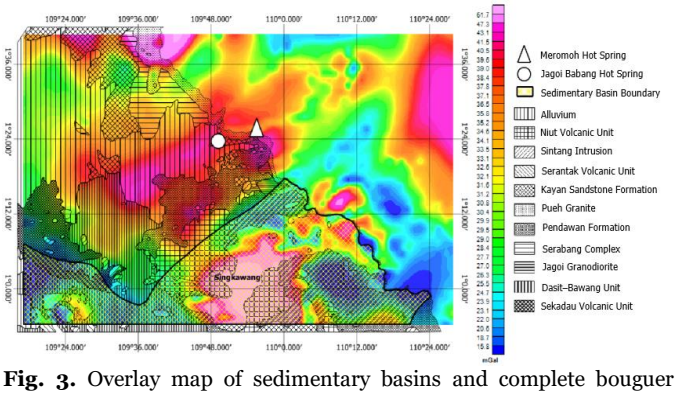

Fig. 3. Overlay map of sedimentary basins and complete bouguer anomaly (CBA) in the Meromoh geothermal area, West Kalimantan, Indonesia.

In Fig. 3, an overlay map of sedimentary basins and ABL can be seen to determine the location of sedimentary basins relative to the Meromoh and Jagoi Babang geothermal fields. The Meromoh and Jagoi Babang geothermal fields are located outside or between sedimentary basins with medium-to-high anomalies. Overlaying the geological map with the sedimentary basin map reveals that the sedimentary basins are filled by formations dominated by mudstone and sandstone. The Meromoh geothermal field is situated within the Pueh Granite Formation, which is dominated by granite rock.

4.2. *Spectral analysis and depth estimation*

Spectral analysis was conducted to estimate the average depth of gravity anomaly sources and to separate regional and residual components prior to structural modeling. The method is based on Fourier transformation, which converts gravity data from the spatial domain into the frequency (wavenumber) domain. In the logarithmic power spectrum, the slope of linear segments is proportional to the depth of the causative sources, following the relationship between exponential decay of anomaly amplitude and source depth [20, 21, 25].

Fig. 4 presents the logarithmic amplitude plotted against wavenumber. The spectrum exhibits two dominant linear segments, indicating the presence of two principal discontinuity levels within the subsurface. The regional anomaly component was separated using a cutoff wavenumber of 0.0595, yielding an estimated average source depth of approximately 3.9 km. This depth is interpreted to represent deeper crustal density contrasts, likely associated with intrusive basement geometry or large-scale lithological variations. The residual anomaly component was separated using a cutoff wavenumber of 0.4629, corresponding to an estimated average depth of approximately 1.7 km. This shallower component reflects localized density variations related to near-surface structures such as fault zones, intrusive contacts, or lithological boundaries.

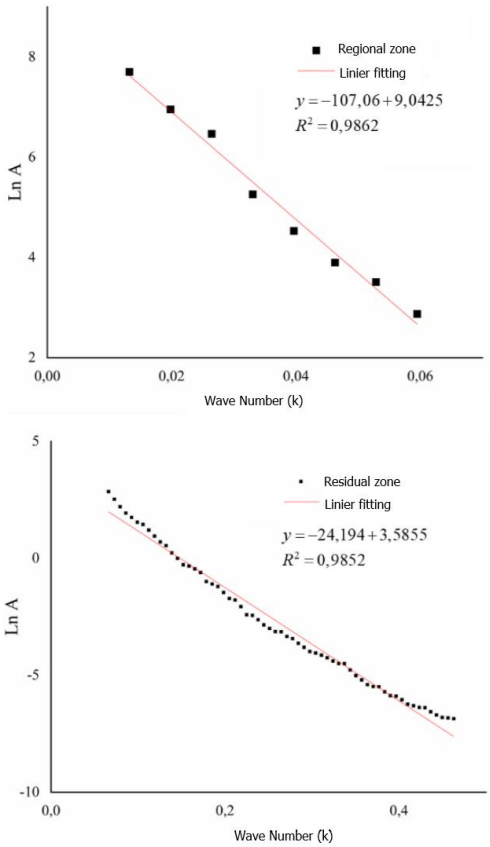

Fig. 4. Curve of spectral analysis of regional anomalies, residuals, and noise separation.

The distinction between these two depth levels suggests a multi-layered subsurface structure beneath the Meromoh geothermal area. The deeper regional component (~3.9 km) may correspond to the upper portion of granitic intrusions or basement highs that influence the regional thermal regime. In contrast, the residual component (~1.7 km) likely represents structurally controlled zones that facilitate hydrothermal circulation and surface geothermal manifestations. The spectral separation provides a quantitative basis for subsequent frequency-domain filtering. By isolating the residual anomaly field, the structural interpretation focuses on shallow features that are directly relevant to geothermal fluid pathways, while the regional component constrains the broader crustal architecture.

The delineation of depth boundaries for both regional and residual components in Fig. 5 was determined based on the coefficient of determination (R^2) obtained from the spectral analysis curves. The variation in R^2 values between linear segments indicates a clear separation between deep-seated (regional) and shallow (residual) anomaly sources. Each linear segment in the logarithmic amplitude versus wavenumber plot represents a distinct discontinuity level within the subsurface structure.

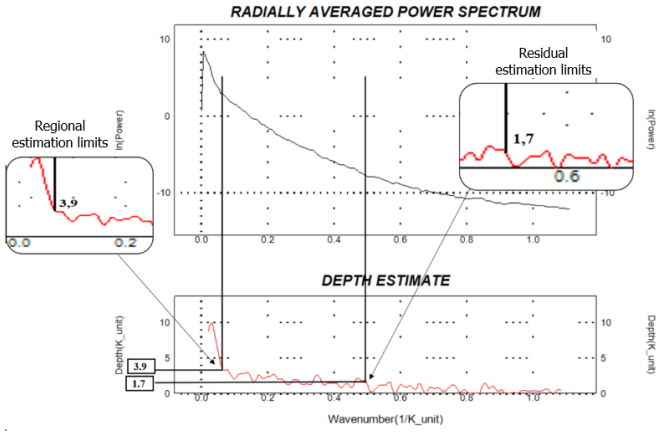

Fig. 5. Analysis and estimation of depth.

Depth estimation of the anomaly sources was carried out by applying Fourier transformation to the Complete Bouguer Anomaly data using Oasis Montaj software. The slope of each linear segment in the log-amplitude versus wavenumber domain was used to calculate the average depth of the corresponding anomaly source. This approach enables a quantitative separation of regional and residual components, thereby improving the reliability of subsequent structural interpretation.

4.3. *Separation of regional and residual anomalies*

Noise-free regional and residual anomaly contour maps were generated through filtering of the Complete Bouguer Anomaly (CBA) dataset. The separation was performed using Butterworth and band-pass filters implemented in Oasis Montaj. The Butterworth filter was applied to isolate the long-wavelength regional component from the total anomaly field, whereas the band-pass filter was used to suppress high-frequency noise within the residual field. This filtering approach enables the separation of deep-seated anomaly sources (regional) from shallow subsurface sources (residual), thereby improving structural interpretation.

As shown in Fig. 6, the regional anomaly map exhibits broader spatial coverage compared to the residual component, with anomaly values ranging from 15.5 mGal to 60.9 mGal. The regional anomaly displays relatively high values in the central and southern parts of the study area, gradually decreasing toward the southeastern sector. The elevated anomaly values in the central and southern regions indicate the presence of higher-density subsurface rocks compared to the southeastern area.

The Meromoh geothermal manifestation is located within a high regional anomaly zone (approximately 40.3–60.9 mGal), represented by pink to red colors. This area corresponds to the Pueh Granite Formation, which is dominated by granitic lithologies. In contrast, the Jagoi Babang geothermal manifestation is situated within a moderately high anomaly zone (approximately 38.9–41.3 mGal), associated with the Kayan Sandstone Formation. This formation consists predominantly of quartz sandstone, interpreted as sedimentary rocks derived from the weathering and erosion of granitic parent rocks. Granite, an intrusive igneous rock typically containing 10–50% quartz, represents the primary source material for these sedimentary deposits [16, 26, 27].

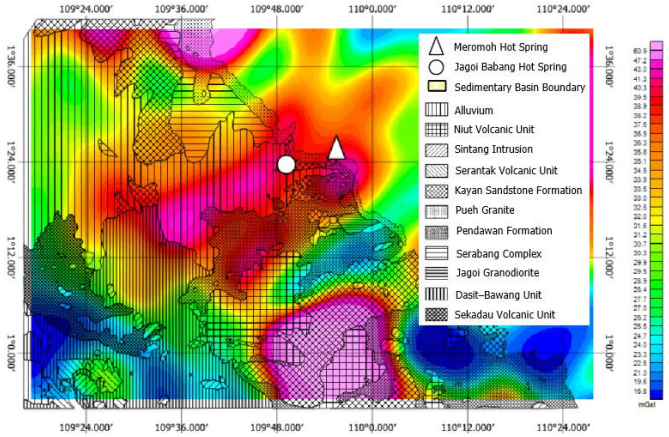

Fig. 6. Regional gravity anomaly map of the Meromoh geothermal area, West Kalimantan, Indonesia.

The residual anomaly map was obtained by subtracting the regional component from the Complete Bouguer Anomaly dataset. As shown in Fig. 7, residual anomaly values range from −6.3 mGal to 5.9 mGal. Low residual anomalies (−6.3 to 0.3 mGal) are interpreted as zones of reduced density, potentially associated with fractured, altered, or weathered rocks that may enhance permeability. High residual anomalies (0.4 to 5.9 mGal) likely correspond to shallow high-density bodies, such as intrusive units or structurally uplifted basement rocks [16, 26, 27].

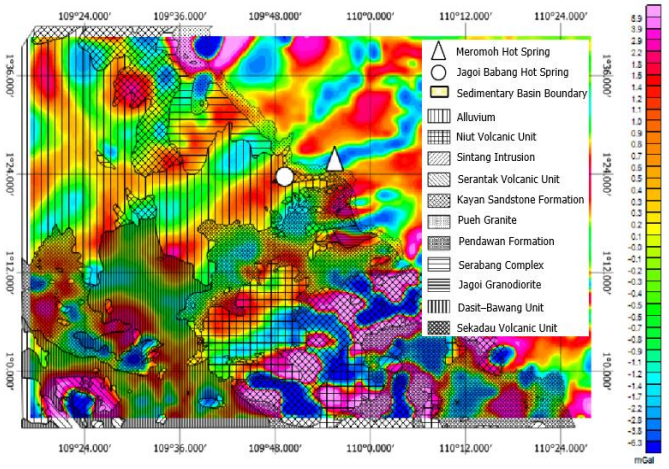

Fig. 7. Residual gravity anomaly map.

It is important to note that gravity measurements are influenced by topographic elevation; higher elevations generally produce lower observed gravity values due to increased distance from the Earth's center of mass [20, 21, 25]. However, after applying Bouguer and terrain corrections, the residual anomaly predominantly reflects subsurface density contrasts rather than topographic effects, thereby providing a more reliable representation of shallow structural variations [16, 26, 27].

4.4. 2D gravity anomaly modeling

Two-dimensional (2D) forward gravity modeling was conducted using the Complete Bouguer Anomaly (CBA) map, constrained by regional geological data. The objective of this stage was to reconstruct subsurface lithological geometry that is consistent with observed gravity responses and known geological formations. Modeling was performed using the GM-SYS module in Oasis Montaj. Three profiles were constructed: A–A′, B–B′, and C–C′ (Fig. 8). Profile A–A′ crosses the Meromoh geothermal manifestation, profile B–B′ intersects the Jagoi Babang geothermal area, and profile C–C′ traverses both geothermal manifestations.

Profile A–A′ extends approximately 90 km with a modeled depth exceeding 12 km. The resulting RMS error for this model is 4.286%, indicating good agreement between observed and calculated gravity anomalies. The subsurface along this profile is interpreted to consist of five principal formations: Kayan Sandstone (Tkk), Pendawan Formation (Kp), Dasit–Bawang Unit (TRJb), Pueh Granite (Kup), and Niut Volcanic Unit (Tpn). The Kayan Sandstone ($\rho \approx 1.82$ g/cm³) consists predominantly of quartz sandstone with minor mudstone and conglomerate. The Pendawan Formation ($\rho \approx 2.40$ g/cm³) comprises Early Cretaceous sedimentary rocks, including shale, siltstone, calcareous mudstone, and minor conglomerate. The Dasit–Bawang Unit ($\rho \approx 2.61$ g/cm³) is composed of volcanic rocks such as lava, breccia, tuff, and agglomerate, with andesitic to basaltic composition and granodioritic intrusions. The Pueh Granite ($\rho \approx 2.76$ g/cm³) consists of granite, granodiorite, and diorite, representing intrusive igneous bodies. The Niut Volcanic Unit forms the upper volcanic sequence.

The Meromoh geothermal manifestation is spatially associated with the Pueh Granite body, which extends to significant depth. The modeled geometry suggests that this intrusive unit may play an important role in the regional thermal framework. Additionally, the model indicates the presence of a structural depression near the geothermal site, potentially facilitating fluid accumulation and circulation. Profile B–B′ extends approximately 120 km with a modeled depth exceeding 12 km and yields an RMS error of 4.656%. The subsurface structure along this profile consists of seven formations: Alluvial Deposits (Qa), Kayan Sandstone (Tkk), Pendawan Formation (Kp), Jagoi Granodiorite (TRJlj), Pueh Granite (Kup), Serantak Volcanic Unit (Tes), and Sintang Intrusion (Toms).

Alluvial deposits ($\rho \approx 1.70$ g/cm³) represent unconsolidated sediments. The Kayan Sandstone ($\rho \approx 1.94$ g/cm³) and Pendawan Formation ($\rho \approx 2.49$ g/cm³) represent sedimentary sequences. Jagoi Granodiorite ($\rho \approx 2.67$ g/cm³), Pueh Granite ($\rho \approx 2.61$ g/cm³), Serantak Volcanic Unit ($\rho \approx 2.76$ g/cm³), and Sintang Intrusion ($\rho \approx 2.83$ g/cm³) represent intrusive and volcanic lithologies of relatively higher density.

The Jagoi Babang geothermal manifestation is interpreted to be structurally controlled and associated with the intrusive complexes at depth. Similar to profile A–A′, the model indicates a localized structural depression that may enhance permeability and fluid flow. Profile C–C′ extends approximately 150 km with a modeled depth exceeding 12 km and yields an RMS error of 4.229%. This profile intersects both geothermal manifestations and includes five main formations: Alluvial Deposits (Qa), Kayan Sandstone (Tkk), Jagoi Granodiorite (TRJlj), Pueh Granite (Kup), and Sekadau Volcanic–Metamorphic Unit (PzTRs).

The Sekadau Unit ($\rho \approx 2.67$ g/cm³) consists of metamorphic rocks such as phyllite, quartzite, gneiss, schist, and migmatite, with minor altered volcanic rocks and amphibolite. The Pueh Granite ($\rho \approx 2.59$ g/cm³) appears as a deep-rooted intrusive body underlying both geothermal areas. Across all profiles, a consistent structural feature is observed: major fault zones (indicated by dashed yellow lines in Fig. 8) intersect the geothermal manifestations. These faults are interpreted as permeable conduits that facilitate fluid migration between deep intrusive bodies and surface hot springs.

Overall, the 2D models suggest that the geothermal system in the Meromoh–Jagoi Babang area is structurally controlled and associated with deep intrusive granitic bodies. However, the presence of high-density granite alone does not confirm active heat production; rather, the interaction between intrusive geometry and fault-controlled permeability is likely the primary factor governing hydrothermal circulation.

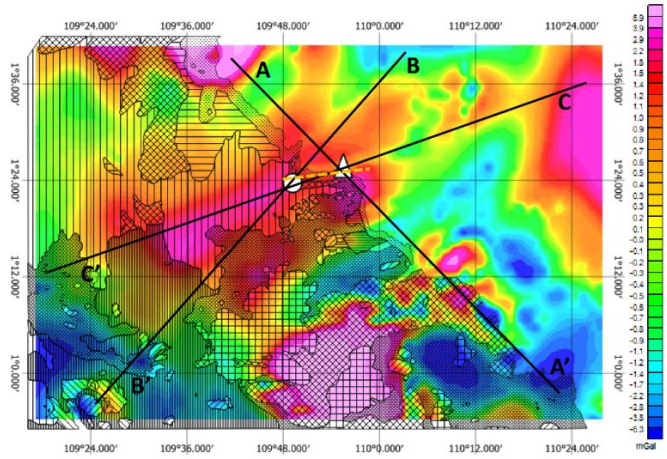

Fig. 8. Integrated geological and Complete Bouguer Anomaly (CBA) map of Belitung Island.

4.5. 3D gravity anomaly modeling

Three-dimensional (3D) gravity modeling was performed to reconstruct the volumetric distribution of subsurface density beneath the Meromoh geothermal area. The modeling was conducted using Grablox 1.6e and visualized in Bloxer 1.6e, based on the Complete Bouguer Anomaly (CBA) dataset. The 3D modeling consisted of two principal stages: forward modeling and inversion modeling. In the forward modeling stage, an initial block model was constructed using gridded CBA data generated in Surfer 15. The model domain was discretized into major and minor blocks, representing the spatial extent and resolution of the study area. Density constraints were assigned based on values obtained from the 2D forward modeling results.

The inversion stage aimed to minimize the misfit between observed and calculated gravity anomalies through iterative optimization. The optimization sequence included base model adjustment, density optimization, Occam density smoothing, elevation adjustment, and Occam height smoothing. These steps ensured that the resulting model achieved both mathematical consistency and geological plausibility. The final 3D model reveals subsurface structures down to a depth of approximately 12–16 km. Density values range between 1.0 and 3.0 g/cm³, reflecting the contrast between unconsolidated sediments, sedimentary formations, metamorphic rocks, and intrusive bodies.

High-density zones are predominantly concentrated in the central and southern sectors of the study area, corresponding to granitic and granodioritic intrusions such as the Pueh Granite and Jagoi Granodiorite. These intrusive bodies appear as vertically extensive features that penetrate through overlying sedimentary and volcanic units. Lower-density zones are associated with sedimentary formations such as the Kayan Sandstone and Pendawan Formation, which likely function as potential reservoir units due to their relatively higher porosity and fracture potential. In addition, localized low-density anomalies may indicate structurally weakened zones or hydrothermal alteration.

The 3D geometry suggests that the Pueh Granite forms a deep-rooted intrusive body extending beneath both the Meromoh and Jagoi Babang geothermal manifestations. However, the presence of intrusive granite alone does not necessarily confirm active heat generation. Instead, the structural configuration and fault systems intersecting these intrusions appear to play a crucial role in controlling hydrothermal fluid migration. Major fault zones, identified in both 2D and 3D models, intersect the geothermal manifestation areas and likely act as permeable pathways connecting deep intrusive bodies to shallow levels. These structural discontinuities enable meteoric water to circulate downward, be heated at depth, and subsequently ascend to the surface as warm springs [16].

Following the forward and inversion modeling stages, the three-dimensional (3D) subsurface model was visualized using Bloxer 1.6e. The final 3D density model of the Meromoh geothermal area is presented in Fig. 9, showing four different viewing perspectives to illustrate the spatial geometry of subsurface structures [16].

The modeled density values range from 1.0 g/cm³ to 4.0 g/cm³, reflecting significant contrasts between sedimentary units, volcanic sequences, metamorphic rocks, and intrusive bodies. The model consists of eight vertical layers extending to a maximum depth of approximately 8.56 km along the Z-axis. Density variations within each block are represented using a color scale, where contrasting colors indicate differences in subsurface lithology and structural configuration.

Rather than relying solely on color representation, interpretation focused on the spatial distribution and continuity of density contrasts within the 3D volume. High-density zones are interpreted as intrusive igneous bodies or basement highs, whereas lower-density zones correspond to sedimentary or fractured units that may act as potential reservoirs.

To facilitate structural interpretation, two representative depth slices along the Z-axis were selected. These slices were chosen to capture the overall geometry of the intrusive bodies and surrounding formations at both shallow and intermediate depths. This approach allows visualization of lateral density variations and their relationship to geothermal manifestations, providing insight into the structural controls governing hydrothermal circulation.

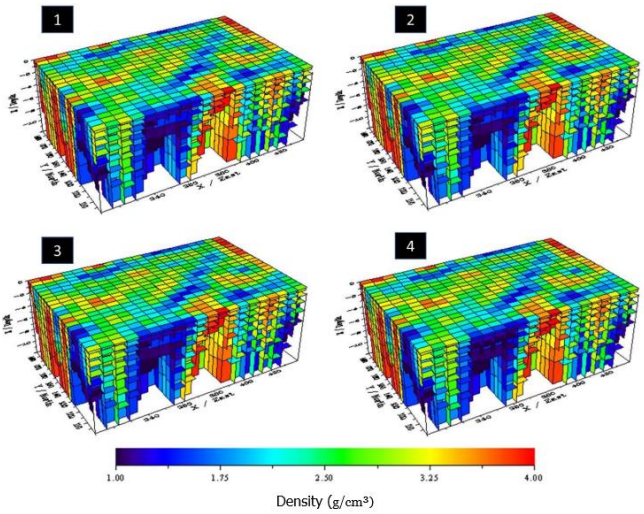

Fig. 9. 3D subsurface model of the Pemali geothermal area.

Further interpretation of the 2D forward modeling results along profile A–A′ (Fig. 10) indicates that the Meromoh geothermal area is composed of several major lithological units, including the Kayan Sandstone Formation, Pendawan Formation, Dasit–Bawang Formation, Pueh Granite, and Niut Volcanic Formation. Each formation exhibits distinct density contrasts consistent with the gravity anomaly response. The Kayan Sandstone Formation is characterized by a relatively low density of approximately 1.82 g/cm³, extending to a depth of ~2.5 km. This unit is interpreted as a sedimentary cover composed predominantly of quartz sandstone with minor mudstone and conglomerate. Beneath this unit, the Pendawan Formation exhibits an average density of 2.40 g/cm³, extending to approximately 4 km depth, consisting mainly of shale, siltstone, and calcareous mudstone.

The Pueh Granite Formation shows a significantly higher average density of 2.76 g/cm³, extending downward to approximately 11.59 km, and is interpreted as the principal heat-conducting body within the system. The relatively high Complete Bouguer Anomaly values in the Meromoh area (40.3–60.9 mGal) correlate strongly with the distribution of this granitic intrusion. These elevated gravity values indicate the presence of dense intrusive bodies at depth. The modeling results suggest that the subsurface structure beneath the Meromoh geothermal manifestation is dominated by granite that ascends through structurally controlled pathways, particularly fault zones. These faults act as conduits for hydrothermal fluid migration, enabling heat transfer from the deep radiogenic granite to shallower permeable formations.

Structural analysis of Fig. 10 reveals the presence of secondary fault structures formed due to tectonic stresses and brittle deformation. These fractures enhance permeability within the otherwise low-porosity

crystalline rocks. The fault zones likely serve as geothermal reservoirs by facilitating meteoric water infiltration. In this system, meteoric water percolates downward through permeable sedimentary layers and fractures, is heated conductively by the underlying granitic body, and then rises back to the surface as warm spring manifestations.

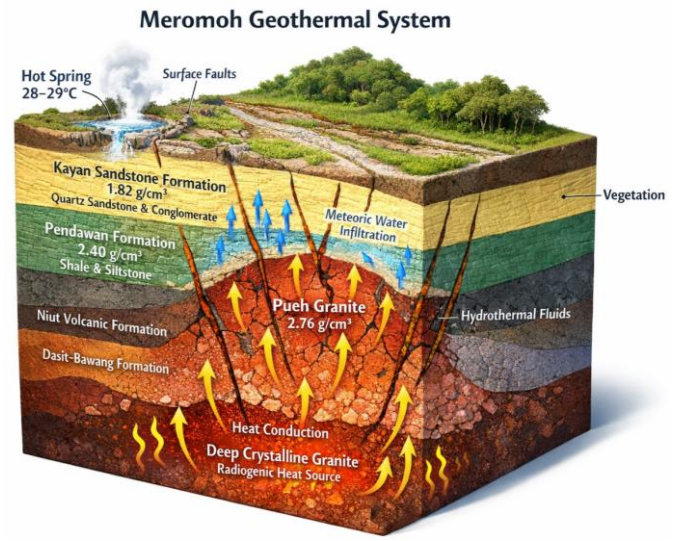

Fig. 10. Integrated conceptual geothermal model of the Buding system, East Belitung, illustrating intrusion-related heat generation and structurally controlled hydrothermal circulation. Deep granitic bodies act as radiogenic heat sources, while folded sedimentary formations serve as permeable reservoirs. Faults and fractures facilitate upward heat transfer and meteoric fluid convection, resulting in hot spring manifestations at the surface.

The measured surface temperature of the Meromoh hot spring (~28–29°C) indicates a low-enthalpy geothermal system. The relatively modest temperature suggests that heat transfer from the granite does not occur through direct contact with groundwater. Instead, heat is transferred indirectly through intermediate sedimentary layers, particularly the overlying Kayan Sandstone Formation, which acts as a transitional heat-transfer medium. This configuration is consistent with a structurally controlled, granite-hosted non-volcanic geothermal system driven primarily by radiogenic heat production rather than active magmatism.

Overall, the integration of density modeling and structural interpretation confirms that the Meromoh geothermal system represents a granite-dominated, fault-controlled, low-temperature geothermal system, where radiogenic heat production within deep intrusive bodies plays a key role in sustaining thermal anomalies. [28, 29].

5. Conclusion

This study presents an integrated interpretation of satellite-derived gravity data combined with 2D forward modeling and 3D inversion to characterize the subsurface structure of the Meromoh geothermal system, West Kalimantan. The Complete Bouguer Anomaly (CBA) map reveals gravity values ranging from 15.8 mGal to 61.7 mGal, indicating significant subsurface density contrasts associated with granitic intrusions and surrounding sedimentary formations. Spectral analysis estimates that the regional anomaly sources occur at an average depth of approximately 3.9 km, while residual anomaly sources are located at shallower depths of around 1.7 km. These results confirm the presence of both deep-seated intrusive bodies and shallow structural heterogeneities influencing the geothermal system. The 2D forward modeling along selected profiles identifies several major lithological units, including the Kayan Sandstone Formation, Pendawan Formation, Dasit–Bawang Formation, and the Pueh Granite Formation. Among these units, the Pueh Granite exhibits the highest density (2.76 g/cm³) and extends to depths of approximately 11.59 km. This granitic body is interpreted as the principal radiogenic heat source within the Meromoh geothermal system. Elevated gravity anomalies (40.3–60.9 mGal) spatially correlate with the distribution of this intrusive body.

Structural analysis indicates that fault zones play a critical role in controlling geothermal fluid circulation. These fractures act as permeability pathways that allow meteoric water to infiltrate downward, absorb heat conductively from the granitic body, and return to the surface as warm spring manifestations. The relatively low surface temperature (~28–29°C) suggests a low-enthalpy, non-volcanic geothermal system dominated by conductive heat transfer rather than direct magmatic input. The 3D inversion model further confirms the dominance of high-density intrusive bodies beneath the study area and reveals a structurally controlled geothermal architecture extending to depths of approximately 8–11 km. The integration of gravity anomaly analysis, spectral depth estimation, and structural modeling provides a coherent conceptual framework for understanding granite-hosted radiogenic geothermal systems in West Kalimantan. Overall, the Meromoh geothermal system is interpreted as a granite-hosted, structurally controlled, low-temperature geothermal system driven by radiogenic heat production within deep intrusive bodies. This study highlights the effectiveness of integrated gravity modeling for reducing exploration uncertainty in non-volcanic geothermal provinces and provides a geophysical basis for future geothermal exploration in granite-dominated regions of Indonesia.

CRediT authorship contribution statement

Succi Angling Situmorang: Writing – review & editing, Writing – original draft, Supervision, Software, Resources, Methodology, Investigation, Formal analysis, Data curation. **Ahmad Said:** Writing – review & editing, Supervision, Resources, Methodology, Investigation, Formal analysis, Data curation, Conceptualization.

Declaration of Competing Interest

The authors declare that they have no known competing financial interests or personal relationships that could have appeared to influence the work reported in this paper.

Data availability

Data will be made available on request.

Acknowledgment

The authors would like to express their sincere appreciation to the Department of Physics, Institut Teknologi Sumatera, for providing research facilities and computational support during data processing and modeling activities. We also thank the Geological Agency of Indonesia and related institutions for providing regional geological information that supported the interpretation of subsurface structures.

References

1. Hosono, T., Hartmann, J., Louvat, P., Amann, T., Washington, K. E., West, A. J., Okamura, K., Böttcher, M. E., and Gaillardet, J. (2018). Earthquake-Induced Structural Deformations Enhance Long-Term Solute Fluxes from Active Volcanic Systems, *Scientific Reports*, Vol. 8, No. 1, 1–12. doi:10.1038/s41598-018-32735-1.

2. Zhang, Z., Yao, H., Wang, W., and Liu, C. (2021). 3-D Crustal Azimuthal Anisotropy Reveals Multi-Stage Deformation Processes of the Sichuan Basin and Its Adjacent Journal of Geophysical Research : Solid Earth, *Journal of Geophysical Research: Solid Earth*, Vol. 127, No. e2021JB023289, 1–17. doi:10.1029/2021JB023289.

3. Liu, S., Suardi, I., Xu, X., Yang, S., and Tong, P. (2021). The Geometry of the Subducted Slab Beneath Sumatra Revealed by Regional and Teleseismic Traveltime Tomography, *Journal of Geophysical Research: Solid Earth*, Vol. 126, No. 1, 1–29. doi:10.1029/2020JB020169.
4. Dewi, K. C. S., Siregar, R. N., Ningati, T. I., Pulungan, Z. N., Indriyawati, A., and Takahashi, H. (2025). Analysis of Subsurface Faults Using 3D Gravity Method Based On Satellite Image Data : Insights into Indo-Australian and Eurasian Plate Subduction in the Formation of An Accretionary Prism, *International Journal of Hydrological and Environmental for Sustainability*, Vol. 4, No. 3, 135–148.
5. Hariyono, E., and S, L. (2018). The Characteristics of Volcanic Eruption in Indonesia, *Volcanoes - Geological and Geophysical Setting, Theoretical Aspects and Numerical Modeling, Applications to Industry and Their Impact on the Human Health*, No. July. doi:10.5772/intechopen.71449.
6. McCaffrey, R. (2009). The Tectonic Framework of the Sumatran Subduction Zone, *Annual Review of Earth and Planetary Sciences*, Vol. 37, 345–366. doi:10.1146/annurev.earth.031208.100212.
7. Hristov, V., Stoyanov, N., Valtchev, S., Kolev, S., and Benderev, A. (2019). Utilization of Low Enthalpy Geothermal Energy in Bulgaria, *IOP Conference Series: Earth and Environmental Science*, Vol. 249, No. 1. doi:10.1088/1755-1315/249/1/012035.
8. Taruna, R. M., and Banyunegoro, V. H. (2018). Earthquake Relocation Using Double Difference Method for 2D Modelling of Subducting Slab and Back Arc Thrust in West Nusa Tenggara, *Jurnal Penelitian Fisika Dan Aplikasinya (JPFA)*, Vol. 8, No. 2, 132. doi:10.26740/jpfa.v8n2.p132-143.
9. Collings, R., Lange, D., Rietbrock, A., Tilmann, F., Natawidjaja, D., Suwargadi, B., Miller, M., and Saul, J. (2012). Structure and Seismogenic Properties of the Mentawai Segment of the Sumatra Subduction Zone Revealed by Local Earthquake Traveltime Tomography, *Journal of Geophysical Research*, Vol. 117, 1–23. doi:10.1029/2011JB008469.
10. Jihad, A., Muksin, U., Syamsidik, and Ramli, M. (2021). Earthquake Relocation to Understand the Megathrust Segments along the Sumatran Subduction Zone, *IOP Conference Series: Earth and Environmental Science*, Vol. 630, 012002. doi:10.1088/1755-1315/630/1/012002.
11. Xu, J., and Kono, Y. (2002). Geometry of Slab, Intraslab Stress Field and Its Tectonic Implication in the Nankai Trough, Japan, *Earth, Planets and Space*, Vol. 54, No. 7, 733–742. doi:10.1186/BF03351726.
12. Kusuhara, F., Kazahaya, K., Morikawa, N., Yasuhara, M., Tanaka, H., Takahashi, M., and Tosaki, Y. (2020). Original Composition and Formation Process of Slab-Derived Deep Brine from Kashio Mineral Spring in Central Japan, *Earth, Planets and Space*, Vol. 72, No. 1. doi:10.1186/s40623-020-01225-y.
13. Malod, J. A., Karta, K., Beslier, M. O., and Zen, M. T. (1995). From Normal to Oblique Subduction: Tectonic Relationships between Java and Sumatra, *Journal of Southeast Asian Earth Sciences*, Vol. 12, Nos. 1–2, 85–93. doi:10.1016/0743-9547(95)00023-2.
14. Li, C. F. (2011). An Integrated Geodynamic Model of the Nankai Subduction Zone and Neighboring Regions from Geophysical Inversion and Modeling, *Journal of Geodynamics*, Vol. 51, No. 1, 64–80. doi:10.1016/j.jog.2010.08.003.
15. Stern, R. J. (2002). Subduction Zones, *Reviews of Geophysics*, Vol. 40, No. 4, 3-1-3–38. doi:10.1029/2001RG000108.
16. Utama, H. W., Mulyasari, R., and Said, Y. M. (2021). Geothermal Potential on Sumatra Fault System To Sustainable Geotourism in West Sumatra, *JGE (Jurnal Geofisika Eksplorasi)*, Vol. 7, No. 2, 126–137. doi:10.23960/jge.v7i2.128.
17. Tabei, T., Hashimoto, M., Miyazaki, S., Hirahara, K., Kimata, F., Matsushima, T., Tanaka, T., Eguchi, Y., Takaya, T., Hoso, Y., Ohya, F., and Kato, T. (2002). Subsurface Structure and Faulting of the Median Tectonic Line, Southwest Japan Inferred from GPS Velocity Field, *Earth, Planets and Space*, Vol. 54, No. 11, 1065–1070. doi:10.1186/BF03353303.
18. Tongkul, F. (2017). Active Tectonics in Sabah – Seismicity and Active Faults, *Bulletin of the Geological Society of Malaysia*, Vol. 64, No. December, 27–36. doi:10.7186/bgsm64201703.
19. Maryanto, S. (2017). Geo Techno Park Potential at Arjuno-Welirang Volcano Hosted Geothermal Area, Batu, East Java, Indonesia (Multi Geophysical Approach), *AIP Conference Proceedings*, Vol. 1908, No. 2017. doi:10.1063/1.5012712.
20. Sujitapan, C., Kendall, J. M., Chambers, J. E., and Yordkayhun, S. (2024). Landslide Assessment through Integrated Geoelectrical and Seismic Methods: A Case Study in Thungsong Site, Southern Thailand, *Heliyon*, Vol. 10, No. 2. doi:10.1016/j.heliyon.2024.e24660.
21. Chambers, J., Holmes, J., Whiteley, J., Boyd, J., Meldrum, P., Wilkinson, P., Kuras, O., Swift, R., Harrison, H., Glendinning, S., Stirling, R., Huntley, D., Slater, N., and Donohue, S. (2022). Long-Term Geoelectrical Monitoring of Landslides in Natural and Engineered Slopes, *Leading Edge*, Vol. 41, No. 11, 768–767. doi:10.1190/tle41110768.1.
22. Whiteley, J. S., Watlet, A., Uhlemann, S., Wilkinson, P., Boyd, J. P., Jordan, C., Kendall, J. M., and Chambers, J. E. (2021). Rapid Characterisation of Landslide Heterogeneity Using Unsupervised Classification of Electrical Resistivity and Seismic Refraction Surveys, *Engineering Geology*, Vol. 290, No. May, 106189. doi:10.1016/j.enggeo.2021.106189.
23. Martinho, E. (2023). *Electrical Resistivity and Induced Polarization Methods for Environmental Investigations: An Overview*, *Water, Air, and Soil Pollution* (Vol. 234), Springer International Publishing. doi:10.1007/s11270-023-06214-x.
24. Kusumayudha, S. B., Lestari, P., and Paripurno, E. T. (2018). Eruption Characteristic of the Sleeping Volcano, Sinabung, North Sumatera, Indonesia, and SMS Gateway for Disaster Early Warning System, *Indonesian Journal of Geography*, Vol. 50, No. 1, 70–77. doi:10.22146/ijg.17574.
25. Meju, M. A., and Le, L. (2002). Geoelectromagneticexploration For Natural Resources:Models, Case Studies and Challenges, *Surveys in Geophysics*, Vol. 23, 133–205.
26. Lange, D., Tilmann, F., Henstock, T., Rietbrock, A., Natawidjaja, D., and Kopp, H. (2018). Structure of the Central Sumatran Subduction Zone Revealed by Local Earthquake Travel-Time Tomography Using an Amphibious Network, *Solid Earth*, Vol. 9, No. 4, 1035–1049. doi:10.5194/se-9-1035-2018.
27. Lin, J. Y., Sibuet, J. C., Hsu, S. K., and Wu, W. N. (2014). Could a Sumatra-like Megathrust Earthquake Occur in the South Ryukyu Subduction Zone?, *Earth, Planets and Space*, Vol. 66, No. 1, 1–8. doi:10.1186/1880-5981-66-49.
28. Siringoringo, L. P., Sapiie, B., Rudyawan, A., and Sucipta, I. G. B. E. (2024). Origin of High Heat Flow in the Back-Arc Basins of Sumatra: An Opportunity for Geothermal Energy Development, *Energy Geoscience*, Vol. 5, No. 3, 100289. doi:10.1016/j.engeos.2024.100289.
29. Hochstein, M. P., and Sudarman, S. (1993). Geothermal Resources of Sumatra, *Geothermics*, Vol. 22, No. 3, 181–200. doi:10.1016/0375-6505(93)90042-L.